Journal of Hazardous Materials 176 (2010) 692–696

Contents lists available at ScienceDirect

Journal of Hazardous Materials

journal homepage: www.elsevier.com/locate/jhazmat

Detection of explosives by positive corona discharge ion mobility spectrometry

Mahmoud Tabrizchi*, Vahideh ILbeigi

Department of Chemistry, Isfahan University of Technology, Isfahan 84156-83111, Iran

ARTICLE INFO

Article history:
Received 9 September 2009
Received in revised form 9 November 2009
Accepted 15 November 2009
Available online 8 December 2009

Keywords:
Explosives
Ion mobility spectrometry
Pyrolysis

ABSTRACT

In this work, thermal decomposition has been used to detect explosives by IMS in positive polarity. Explosives including Pentaerythritol Tetranitrate (PETN), Cyclo-1,3,5-Trimethylene-2,4,6-Trinitramine (RDX), 2,4,6-Trinitrotoluene (TNT), 2,4-Dihydro-5-nitro-3H-1,2,4-triazol-3-one (NTO), 1,3,5,7-Tetranitro-1,3,5,7-tetrazocine (HMX), have been evaluated at temperatures between 150 and 250 °C in positive polarity in air. Explosives yield NO_x which causes NO^+ peak to increase. Additional peaks may be used to identify the type of explosive. The limit of detection for RDX, HMX, PETN, NTO, and TNT were obtained to be 1, 10, 40, 1000, and 1000 ng, respectively.

1. Introduction

The increasing worldwide terrorist threats nowadays have made it crucial to detect all kinds of explosives in order to provide a secure protection for important places such as air ports, embassies, governmental buildings, public and holy places, power stations, dams, etc. Many methods have been reported for the detection of explosives and various techniques have been comprehensively reviewed in the literature. X-ray screening [1], fluorescence quenching [2], neutron and gamma-ray spectroscopy [3], LC–MS [4], UV gated Raman spectroscopy [5], laser induced breakdown spectroscopy (LIBS) [6], electrochemical and immunosensors [7], chemiluminescence [8], SPME-HPLC [9], and GC-ECD [10,11] are among the new methods proposed for explosive detection. Recently, metal oxide semiconductor (MOS) nanoparticle sensors [12] have been used for the detection and discrimination of low concentrations of explosives.

Ion mobility spectrometry (IMS) has proved to be one of the best methods for the detection of trace level of explosives due to its low detection limit, fast response, simplicity, and portability. IMS based instruments are now vastly used in vulnerable places such as airports for screening of both people and carry-on luggage. A critical review of ion mobility spectrometry for the detection of explosives and explosive-related compounds up to 2001 is given by Ewing et al. [13]. Buxton et al. applied rapid multivariate curve resolution for identification of explosives by IMS [14]. Hill et al. constructed a high-flow, high-resolution ion mobility spectrometer for the detection of explosives after personnel portal sampling [15]. Determination of explosives in water samples was reported by Lokhnauth et al. [16].

Ion mobility spectrometry is basically a gas-phase ion separation technique that operates under atmospheric pressure. A full description of the method is given in books and review articles [17–20]. A drift tube consisting of a reaction region and a drift region is the main element of the ion mobility spectrometer. An electric field is created by a series of conducting guard rings. The analyte vapor is introduced by an inert gas into the reaction region where the analyte molecules are ionized at atmospheric pressure via ion-molecule reactions. The ions are then injected to the drift region by an ion shutter where they move towards the end of the tube where they, finally, strike the collector plate. Ions of different identities are separated due to different velocities arising from their intrinsic mobilities. The ion current is amplified with a fast electrometer and then recorded versus time to make an ion mobility spectrum. IMS may operate in two different modes, positive or negative. In the positive mode, only positive ions are detected while, in the negative mode, the electric field is reversed to collect the negative ions. Explosives are commonly detected in the negative mode. Normally, an electron source is used for the ionization in the negative mode. Ionization of the analyte takes place via electron capture or negative ion attachment reactions. The excellent sensitivity of IMS to explosives is due to its very high electron affinity. The ionization source of the conventional IMS is a radioactive ^{63}Ni foil which emits high energy electrons. For instruments that use the ambient air as the carrier gas, electrons are mostly captured by oxygen, hence producing negative reactant ions, Eq. (1). Explosives containing nitro groups, with electron affinity higher than that of oxygen, are then ionized according to Eq. (2).

$$e + O_2 \rightarrow O_2^- \quad \text{orotherreactantions} \tag{1}$$

* Corresponding author. Tel.: +98 311 3913272; fax: +98 311 3912350.
E-mail address: m-tabriz@cc.iut.ac.ir (M. Tabrizchi).

0304-3894/$ – see front matter © 2009 Elsevier B.V. All rights reserved.
doi:10.1016/j.jhazmat.2009.11.087

$$R\text{–}NO_2 + O_2^- \rightarrow R\text{–}NO_2^- + O_2 \quad (2)$$

The advantages of ^{63}Ni are simplicity, stability, being noise-free, and no requirement for extra power for ionization. However, there are serious problems associated with using radioactive materials. Usually working with such materials needs regular leak test and special safety regulations. Licensing and waste disposal are also required which limits the acceptance of IMS instruments in the market place. Several alternative ionization sources have been reported including UV light [21,22], corona discharge [23], and pulsed discharge [24]. An excellent electron source, particularly for the negative IMS, was developed in our lab [25]. The source utilizes a discharge in pure nitrogen which produces electrons, several orders of magnitude higher than that produced by the conventional ^{63}Ni. An IMS equipped with such source was demonstrated to be very sensitive to trace levels of explosives [26]. In spite of its very good performance, the electron source needs pure nitrogen for its operation. Thus, the source may not be convenient to be used in the portable instruments. If negative corona discharge happens in air, it produces NO_2^- with a very high electron affinity, even higher than that of explosives, and prevents ionization of those compounds. Thus, negative corona discharge in air is not appropriate for the detection of explosives.

The aim of this work is to use the positive corona discharge operating in air for ionization of explosives. This was achieved by considering the pyrolysis of explosives at elevated temperatures. The products of the pyrolysis contain nitrogen oxide that is well ionized in the positive corona discharge. As a result, explosives may be detected by monitoring the NO^+ peak in ion mobility spectrum. Moreover, each explosive shows additional peaks that may be used for identification.

2. Experimental

2.1. Instrumentation

The IMS used in this study was constructed in our laboratory at Isfahan University of Technology. An IMS cell (installed in an oven), a needle for producing the corona, two high voltage power supplies, a pulse generator, an analog to digital converter, and a computer to record spectra comprised the main components of the instrument. The ionization region consisted of five thick aluminum rings, with 20 mm ID and 55 mm OD. The drift tube consisted of 11 aluminum rings with the same OD size and 36 mm ID. Each ring was connected to the adjacent one via a 5 MΩ resistor to create a potential gradient. A voltage of 7 kV was applied over the entire cell to create a drift field of 466 V/cm.

The cell temperature could be adjusted from room temperature up to 200 °C. The injection port consisted of an aluminum tube connected to a T-shape swagelok fitting. It could be heated up to 250 °C to enable pyrolysis of explosives. Air was used as carrier and drift gases with flow rate of 400 cm^3/min and 700 cm^3/min. The optimized experimental conditions for the detection of explosives are given in Table 1.

Table 1
The optimized experimental conditions for explosives of detection.

Parameter	Setting
Length of drift tube	11 (cm)
Drift field	466 (V/cm)
Corona voltage	2300 (V)
Flow rate of drift gas (Air)	700 (mL/min)
Flow rate of carrier gas (Air)	400 (mL/min)
Injection port temperature	220 (°C)
IMS cell temperature	200 (°C)

2.2. Materials and methods

Industrial grades of the explosives; pentaerythritol tetranitrate (PETN), cyclo-1,3,5-trimethylene-2,4,6-trinitramine (RDX), 2,4,6-trinitrotoluene (TNT), 2,4-dihydro-5-nitro-3H-1,2,4-triazol-3-one (NTO), 1,3,5,7-tetranitro-1,3,5,7-tetrazocine (HMX) were prepared from Isfahan Chemical Industry (Zarinshahr/Iran). Samples were solved in methanol to make standard solutions. Working standard solutions were prepared by consecutive dilutions of the standard solutions. 10 μL of the working solution was loaded on the injection port and the solvent was allowed to evaporate. NO and NO_2 were produced via reaction between diluted and concentrated nitric acid with Cu, respectively.

3. Results and discussion

3.1. Positive ion mobility spectra of explosives

Positive ion mobility spectrum of NTO along with the background spectrum and the NO_2 spectrum are shown in Fig. 1. The spectra were obtained under the optimized experimental conditions given in Table 1. In the background spectrum, the reactant ions were water clusters of NH_4^+, NO^+, and H_3O^+, respectively. In the NO_2 spectrum, the NO^+ peak increased. It should be mentioned that injecting NO also gave rise to an increase in the NO^+ peak. It is clear that in the NTO spectrum, the NO^+ peak increased considerably with respect to the background spectrum. This is surely the result of releasing NO or NO_2 after pyrolysis. It has been shown that the pyrolysis product of explosives which contain NO_2 or NO group in the range of 180-250 °C are CO_2, CO, NO_2, NO, HONO, H_2O, N_2, CH_2O, and N_2O [27]. We tried to observe ion mobility of all those products. Only NO, NO_2, and HONO increased the NO^+ peak. Thus, the increase in the NO^+ peak represents the presence of NTO. Other explosives, TNT, RDX, HMX, and PETN also showed similar behavior. Their positive spectra are shown in Fig. 2.

It should be mentioned that the extent of increasing the NO^+ peak differs for different explosives in the order HMX > NTO > RDX > TNT > PETN. It was also proved that the NO^+ peak intensity depends on the level of moisture in the carrier gas.

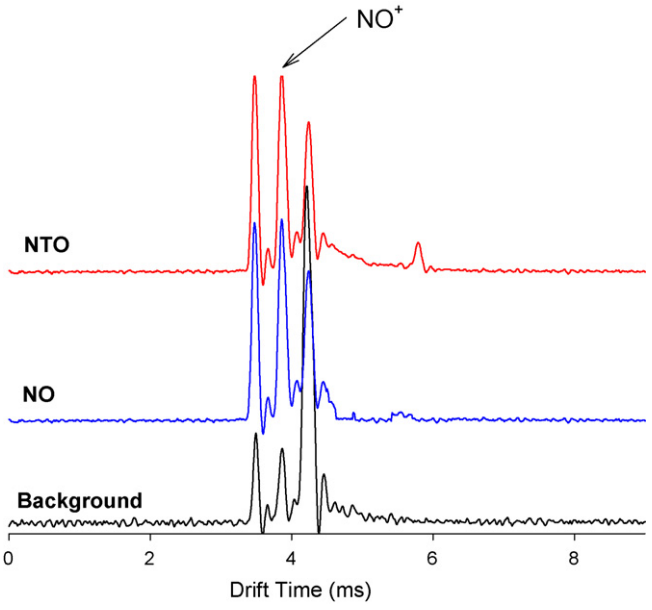

Fig. 1. Positive ion mobility spectra of NTO and NO along with the background spectrum.

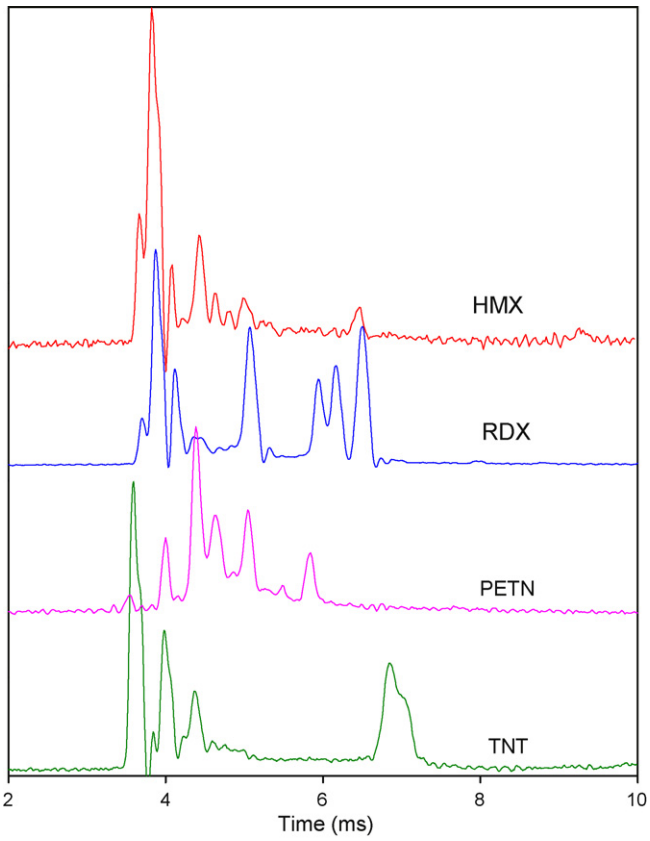

Fig. 2. Positive ion mobility spectra of TNT, RDX, HMX and PETN.

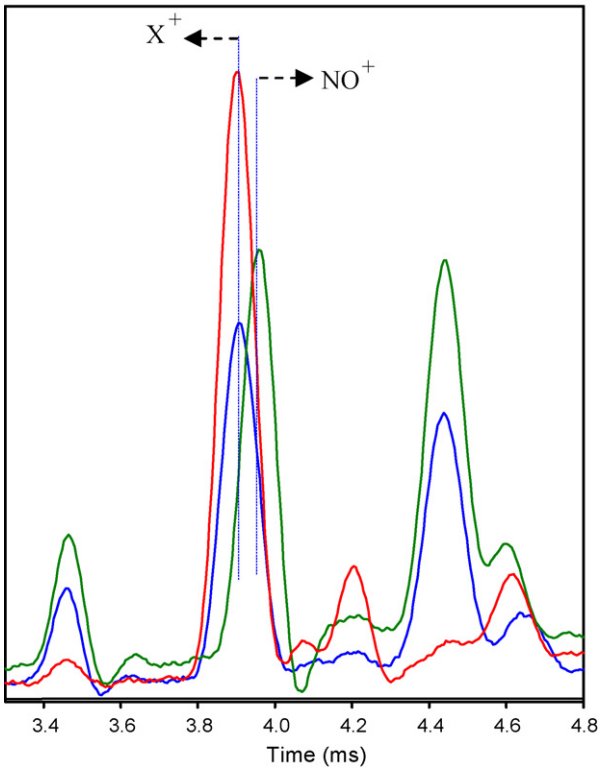

Fig. 3. Comparison of ion mobility spectra of RDX and HMX with that of NO. The X^+ peak appears 0.045 ms before the NO^+ peak.

At high levels of water vapor (>400 ppm), the NO intensity of the explosives was not noticeable.

As shown in Figs. 1 and 2, explosives may be detected by monitoring the NO^+ peak in their ion mobility spectrum. Moreover, each explosive compound shows additional peaks that may be used for identification. For example, RDX and TNT have different patterns, as demonstrated in Fig. 2.

Close examination of the spectra revealed that for HMX and RDX, rather than the NO^+ peak, another peak appears that is very close to the NO^+ peak. Fig. 3 compares the two peaks for RDX, HMX, and NO. The origin of this peak, denoted as X^+, is not clearly known. It appears for only 0.045 ms before the NO^+ peak ($t_X/t_{NO} = 0.989$). Such a small difference was observed because of the high resolution of our instrument. Such high resolution was achieved because of the high ion current produced by the corona discharge which allowed applying a narrow pulse to the shutter grid. In addition a strong voltage (7 kV) was applied to the drift tube to enhance resolution. This experiment was carefully repeated several times to make sure that the X^+ peak differed from the NO^+ peak. Most possible pyrolysis products including HCN, CH_2O, and N_2O were tried and none gave the X^+ peak. This different behavior could be due to the difference in structure among the explosives tested. RDX and HMX yielding the X^+ peak contain an N–NO_2 bond while TNT, NTO, and PETN yielding the NO^+ peak contain either a C–NO_2 or O–NO_2 bond in their structure. To determine the X^+ peak exactly, a mass spectrometer coupled with an IMS is required.

3.2. Reducing the background NO^+ peak

It is well-known that corona discharge in air produces NO^+ and NO_x [28,29]. It has also been empirically established that corona discharge produces a relatively strong wind from the needle tip. The wind carries the neutral nitrogen oxide into the ionization region. NO_x reacts with H_3O^+ and NH_4^+ to produce NO^+. Hence, a source of NO^+ in the ion mobility spectrometry equipped with corona discharge is the neutral NO_x produced in the discharge. As for explosives for which the NO^+ peak is monitored, it is necessary to eliminate, or at least reduce, the background NO^+ peak. The new design consisted of a curtain plate to prevent the diffusion of NO_x into the ionization region as demonstrated in Fig. 4. The curtain plate, mounted in front of the needle, is a metal disk with a hole 2 mm in diameter at its center. A unidirectional flow system was chosen to establish a gas stream just in front of the needle tip to blow it away. This stream prevents the diffusion of NO_x from the discharge region to the ionization region. A voltage is applied to the disk in order to extract reactant ions from the discharge region towards the ionization region.

Although the curtain plate reduced the total intensity of the reactant ions, the intensity of the NO^+ peak relative to that of H_3O^+ reduced considerably. It was noted that the relative intensity of the NO^+ peak depended on the needle voltage as well as on the total flow rate of the gas (carrier + drift). The intensity of the NO^+ peak as a function of the gas flow rate and the needle voltage for both

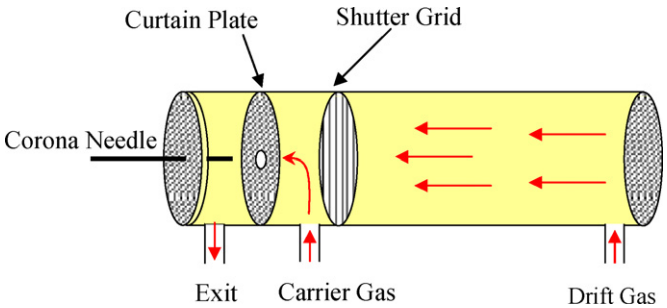

Fig. 4. New design for corona discharge ionization source to eliminate the background NO^+ peak.

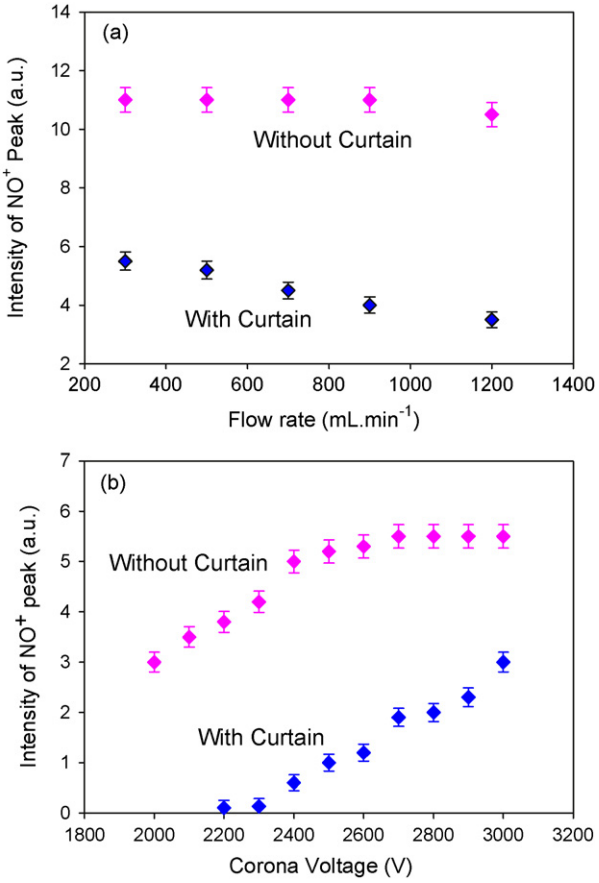

Fig. 5. The intensity of the NO^+ peak versus a) the total gas flow rate and b) the needle voltages, with and without curtain plate.

cases, with and without the curtain plate, is shown in Fig. 5. When the curtain plate is used, the higher flow rate of gas causes less of the NO_x produced in the discharge region to diffuse into the ionization region. This is while in the absence of the curtain plate, the flow rate has no effect. Fig. 5b demonstrates that the NO^+ intensity increases with the needle voltage for both cases, with and without the curtain plate. It has been previously observed that NO^+ production increased with needle voltage. The same trend is observed here. In addition, a higher needle voltage produces a stronger wind

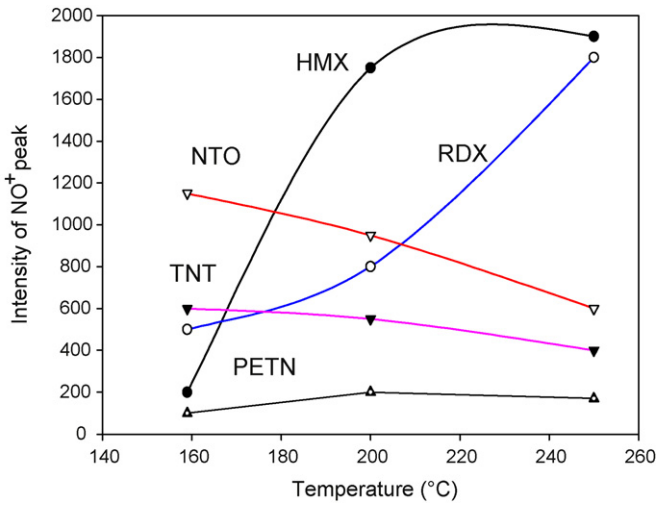

Fig. 6. Intensity of the NO^+ or X^+ peak as a function of pyrolysis temperature.

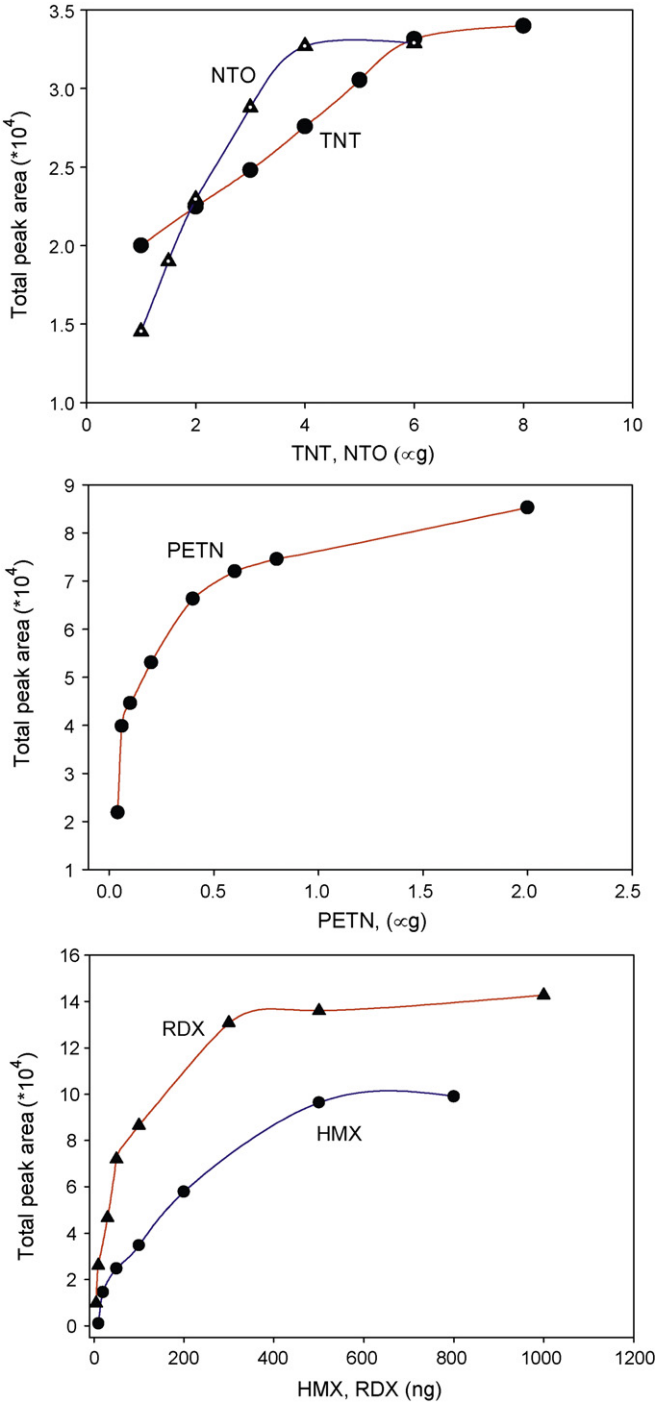

Fig. 7. Calibration curves for RDX, HMX, PETN, NTO, TNT.

which pushes the NO_x into the ionization region. Fig. 5b shows that the NO^+ peak disappears upon reducing the needle voltage, only when the curtain electrode is used.

3.3. *Effect of temperature*

As the most intense peak after the pyrolysis of explosives is the NO^+ peak, the effect of pyrolysis temperature on this peak was explored. This was achieved by recording the spectra for a fixed amount of the sample at different pyrolysis temperatures. Fig. 6 shows the intensity of the NO^+ peak as a function of pyrolysis temperature. In the case of HMX and RDX, the NO^+ peak increases while

it decreases for TNT and NTO. This different behavior could be due to the difference in structure among the explosives tested. As previously described, RDX and HMX contain an N–NO_2 bond form one group with similar temperature behavior. While TNT and NTO contain C–NO_2 bond in their structure form a second group that their NO^+ peak decrease with temperature. PETN which shows different temperature behavior, other than the two groups, contains O–NO_2. The optimum temperature for all explosives is found to be between 200 and 220 °C.

3.4. Calibration curves

The calibration curves for explosives were obtained under optimized conditions given in Table 1 and using the curtain plate. All the calibration curves are shown in Fig. 7. The area under all corresponding peaks for a given sample was considered as the response. The limit of detection, defined as the amount giving peak height three times the noise level, for RDX, HMX, PETN, NTO, and TNT were obtained to be 1, 10, 40, 1000 and 1000 ng, respectively. The order of detection limits is different from that of the increasing NO^+ peak since additional peaks were included in the response and their intensities were different for various substances. The detection limits obtained in this work is generally higher that those values previously published using negative ^{63}Ni-IMS [30] or electrospray [31] and negative corona discharge in nitrogen [26]. However, the advantage of this method over the conventional techniques is that it does not need radioactive sources or nitrogen and is easier and faster with respect to electrospray IMS.

4. Conclusions

In this work, we demonstrated that common explosives can be detected in the positive mode of ion mobility spectrometry with a reasonable detection limit. After modification of the instrument to eliminate the background NO^+ peak, it was found that the presence of explosives could be readily announced by observing the NO^+ peak. In addition, the nature of the explosives may also be determined using the additional peaks. No interference was observed from similar compounds such as pyrazine, dioxane and morpholine which lack NO_2 functional group but contain nitrogen or oxygen atoms.

Generally, portable ion mobility instruments detect narcotics in the positive mode, and explosives in the negative mode. This technique combines detection of both explosives and narcotics in a single mode which makes the instrumentation and operation much simpler. This could be an important progress in the development of portable IMS instruments.

References

[1] Y. Yang, Y. Li, H. Wang, T. Li, B. Wu, Explosives detection using photoneutrons produced by X-rays, Nucl. Instrum. Methods A 579 (2007) 400–403.
[2] M.S. Meaney, V.L. Mcguffin, Investigation of common fluorophores for the detection of nitrated explosives by fluorescence quenching, Anal. Chem. Acta 610 (2008) 57–67.
[3] M. Farahmand, A.J. Boston, A.N. Grint, P.J. Nolan, M.J. Joyce, R.O. Mackin, B.D. Mellow, M. Aspinall, A.J. Peyton, R. Van Silfhout, Detection of explosive substances by tomographic inspection using neutron and gamma-ray spectroscopy, Nucl. Instrum. Methods B 261 (2007) 396–400.
[4] E. Holmgren, H. Carlsson, P. Goedea, C. Crescenzi, Determination and characterization of organic explosives using porous graphitic carbon and liquid chromatography–atmospheric pressure chemical ionization mass spectrometry, J. Chromatogr. A 1099 (2005) 127–135.
[5] M. Gaft, L. Nagli, UV gated Raman spectroscopy for standoff detection of explosives, Opt. Mater. 30 (2008) 1739–1746.
[6] J.L. Gottfried, F.C. De Lucia Jr., C.A. Munson, A.W. Miziolek, Laser-induced breakdown spectroscopy for detection of explosives residues: a review of recent advances, challenges, and future prospects, Anal. Bioanal. Chem. 395 (2) (2009) 283–300.
[7] S. Singh, Sensors—an effective approach for the detection of explosives, J. Hazard. Mater. 144 (2007) 15–28.
[8] A.M. Jimenez, M.J. Navas, Chemiluminescence detection systems for the analysis of explosives, J. Hazard. Mater. 106 (1) (2004) 1–8.
[9] G.V. Kaur, A.K. Kumar, P.K. Malik, K. Rai, SPME-HPLC: a new approach to the analysis of explosives, J. Hazard. Mater. 147 (3) (2007) 691–697.
[10] M.E. Walsh, Determination of nitroaromatic, nitramine, and nitrate ester explosives in soil by gas chromatography and an electron capture detector, Talanta 54 (2001) 427–438.
[11] S Calderara, D. Gardebas, F. Martinez, Solid phase micro extraction coupled with on-column GC/ECD for the post-blast analysis of organic explosives, Forensic Sci. Int. 137 (2003) 6–12.
[12] Y. Guia, C. Xieb, J. Xu, G. Wanga, Detection and discrimination of low concentration explosives using MOS nanoparticle sensors, J. Hazard. Mater. 164 (2009) 1030–1035.
[13] R.G. Ewing, D.A. Atkinson, G.A. Eiceman, G.J. Ewing, A critical review of ion mobility spectrometry for the detection of explosives and explosive related compounds, Talanta 54 (3) (2001) 515.
[14] T.L. Buxton, P.B. Harrington, Rapid multivariate curve resolution applied to identification of explosives by ion mobility spectrometry, J. Anal. Chem. Acta 434 (2001) 269–282.
[15] H.H. Hill, C. Wu, W.E. Steiner, P.S. Tornatore, L.M. Matz, W.F. Siems, D.A. Atkinson, Construction and characterization of a high-flow, high-resolution ion mobility spectrometer for detection of explosives after personnel portal sampling, Talanta 57 (2002) 123–134.
[16] J.K. Lokhnauth, N.H. Snow, Stir-bar sorptive extraction and thermal desorption-ion mobility spectrometry for the determination of trinitrotoluene and 1,3,5-trinitro-1,3,5-triazine in water samples, J. Chromatogr. A 1105 (2006) 33–38.
[17] G.A. Eiceman, Z. Karpas, Ion Mobility Spectrometry, second ed., CRC Press, Boca Raton, 2005.
[18] T.W. Carr, Plasma Chromatography, Plenum Press, New York, 1984.
[19] G.A. Eiceman, Advances in ion mobility spectrometry, Crit. Rev. Anal. Chem. 22 (1991) 17–36.
[20] C.S. Creaser, J.R. Griffiths, C.J. Bramwell, S. Noreen, C.A. Hill, C.L.P. Thomas, Ion mobility spectrometry, a review, Part 1. Structural analysis by mobility measurement, Analyst 129 (2004) 984–994.
[21] M.A. Baim, R.L. Eatherton, H.H. Hill, Ion mobility detector for gas chromatography with a direct photoionization source, J. Anal. Chem. 55 (1983) 1761–1766.
[22] C.S. Leasure, M.E. Fleischer, G.K. Anderson, G.A. Eiceman, Photoionization in air with ion mobility spectrometry using a hydrogen discharge lamp, J. Anal. Chem. 58 (11) (1986) 2142–2147.
[23] M. Tabrizchi, T. Khayamian, N. Taj, Design and optimization of a corona discharge ionization source for ion mobility spectrometry, Rev. Sci. Instrum. 71 (2000) 2321–2328.
[24] Y. An, R. Aliaga Rossel, P. Choi, J.P. Gilles, Development of a short pulsed corona discharge ionization source for ion mobility spectrometry, Rev. Sci. Instrum. 76 (2005) 85105–85111.
[25] M. Tabrizchi, A. Abedi, A novel electron source for negative ion mobility spectrometry, Int. J. Mass Spectrom. 218 (2002) 75–85.
[26] M. Tabrizchi, T. Khayamian, M.T. Jafari, Analysis of 2,4,6-trinitrotoluene, pentaerythritol tetranitrate and cyclo-1,3,5 trimethylene-2,4,6-trinitramine usingnegative corona discharge ion mobility spectrometry, Talanta 59 (2) (2003) 327–333.
[27] C.J. Wu, L.E. Fried, First principles study of high explosive decomposition energetics, in: Eleventh International Detonation Symposium Snowmass, CO, August 31th–September 4th, 1998, p. 8167.
[28] M. Pavlik, J.D. Skalny, Generation of $[H_3O]^+\cdot(H_2O)_n$ clusters by positive corona discharge in air, Rapid Commun. Mass Spectrom. 11 (16) (1997) 1757–1766.
[29] N. Rehbein, V. Cooray, NO_x production in spark and corona discharges, J. Electrostat. 51–52 (2001) 333–339.
[30] D.D. Fetterolf, T.D. Clark, Detection of trace explosive evidence by ion mobility spectrometry, J. Forensic Sci. 38 (1992) 28–39.
[31] H.H. Hill, G.R. Asbury, J. Klasmeier, Analysis of explosives using electrospray ionization ion mobility spectrometry (ESI:IMS), Talanta 50 (2000) 1291–1298.